Nonstationary Oblique Shock-Wave Reflections: Actual Isopycnics and Numerical Experiments

G. Ben-Dor* and I. I. Glass†
University of Toronto, Toronto, Ontario, Canada

Oblique shock-wave reflections in nitrogen for perfect and imperfect gases were investigated interferometrically in a 10- × 18-cm shock tube. Comparisons are made with numerical experiments conducted by two different groups on regular and single-Mach reflections. Even though the analyses are for inviscid flows, the sidewall boundary-layer effects in the experiments are negligible, and the features of the calculated and actual inviscid flows are compared readily. It is found that the available numerical techniques will have to be modified or new approaches developed before acceptable agreement can be obtained between actual and numerical experiments. The very accurate interferometric data will provide a basis for comparison with future numerical methods, which also should include the two remaining cases of complex- and double-Mach reflections as a test of their accuracy and applicability.

Introduction

THE reflections of oblique shock waves in steady flows (supersonic wind tunnels) and nonstationary flows (shock tubes) have been investigated theoretically and experimentally for over three decades.[1-24] During the course of our larger study on the flow regions and transition boundaries[24] of the four basic types of nonstationary oblique shock-wave reflections (Fig. 1), it became apparent that it was important to have a comparison of actual isopycnics and those that have been predicted by numerical methods. A comparison of this nature then would establish the validity and accuracy of the computational techniques to predict such complex shock-wave flows, which is of considerable importance to the fluid-dynamics research community. For, if the numerical results accurately predict the flowfield properties, then many more physical data can be derived numerically than from actual experiments. For example, whereas very accurate lines of constant density (isopycnics) can be obtained from interferograms of the various reflections, the computer outputs can provide pressure, temperature, flow velocity, and other required contours readily. However, a comparison of our specially designed experiments to duplicate the initial conditions in the numerical analyses of Schneyer,[21] Kutler and Shankar,[22] and Shankar et al.[23] showed very satisfactory agreement with the overall wave shapes and systems but unsatisfactory agreement between the more sensitive criterion of the actual isopycnics for the three comparison experiments and those predicted by using different numerical techniques for the available cases of regular and single-Mach reflections. No numerical data presently exist for the complex- and double-Mach-reflection cases. The results presented here and in Ref. 24 represent the most extensive and complete experimental data available at the present time for the four basic types of nonstationary oblique shock-wave reflections. From the discussions and results of Refs. 21-23, there is little doubt that the works of Kutler and Shankar[22] and Shankar et al.[23] provide much more detailed information on flow properties, shock shapes, and their locations, as well as the discovery of vortical singularities, which were not reported previously by other computational fluid dynamicists. However, they may be very optimistic in claiming that their method[22] "is capable of accurately predicting the inviscid flowfield with its single peripheral shock wave and vortical singularity," for regular reflection, and of[23] "accurately predicting the inviscid flow field with its reflected shock, Mach stem and slip surface," for single-Mach reflection. By comparison, Schneyer recognizes the importance of experimental substantiation of any numerical computation by noting,[21] for example, that "final proof of whether the observed curves are or are not slip lines must await detailed comparisons of a calculation with experiment." Consequently, at this time, interferometric isopycnics can be considered more reliable than the corresponding numerical data for inviscid nonstationary flow with shock-wave reflections.

The reader can readily judge the adequacy of the numerical results by comparison with the actual isopycnics. Many more of them could easily have been drawn. Their locations in the (x,y) plane are accurate and have a maximum error of ± 1 mm (0.05-0.1 fringe) and maximum density errors that are fixed for a given initial pressure and temperature. For example, at an initial pressure of 50 Torr and 300 K, the error in density compared to the initial density is 4%, and at 15 Torr (smaller fringe shifts) it can be as high as 13%.

We have shown[24] that ten diffraction regions can exist in a diatomic gas such as nitrogen composed of the four basic reflections RR, SMR, CMR, DMR shown in Fig. 1, depending on the initial shock Mach number M_s and the corner wedge angle θ_w. The transition boundaries depend on whether the gas is perfect or imperfect. Contrary to Shankar et al.,[23] it is possible to obtain SMR, CMR, and DMR from RR for wedge angles in the approximate range $50 \text{ deg} > \theta_w > 45 \text{ deg}$, as the shock Mach number increases from $1 < M_s < 10$, for example, for imperfect nitrogen at an initial pressure of 15 Torr and 300 K.[24] In nonstationary flow, the diffraction process consists of two elements: the reflection of the traveling shock wave incident on the wedge surface, and the deflection by the wedge of the induced flow behind the shock wave, which can be subsonic, transonic, or low supersonic. However, in steady flows only RR and SMR can occur.[24]

It is noteworthy that White[8] in 1951 had already established the existence of the four types of nonstationary oblique shock-wave reflections. His excellent interferograms enabled him to plot isopycnics at low incident shock Mach numbers for regular and single-Mach reflections. Since that time, our interferometric results appear to be the only other data available on the subject.

Experimental Results

The experiments were performed in the University of Toronto Institute for Aerospace Studies (UTIAS) 10 × 18-cm Hypervelocity Shock Tube.[25-28] A 23-cm-diam Mach-Zehnder

Received Oct. 28, 1977; revision received July 24, 1978.

Index categories: Shock Waves and Detonations; Computational Methods.

*Research Assistant, Institute for Aerospace Studies.
†Professor, Institute for Aerospace Studies. Fellow AIAA.

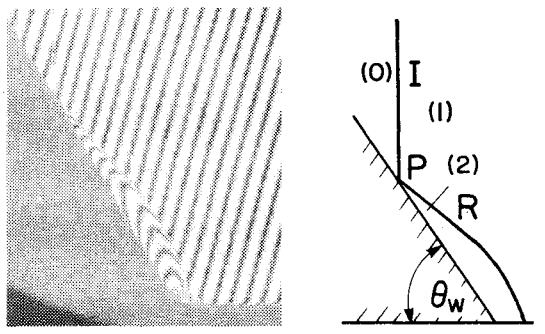

a) Regular reflection (RR), wedge angle $\theta_w = 60$ deg, shock Mach number $M_s = 4.71$.

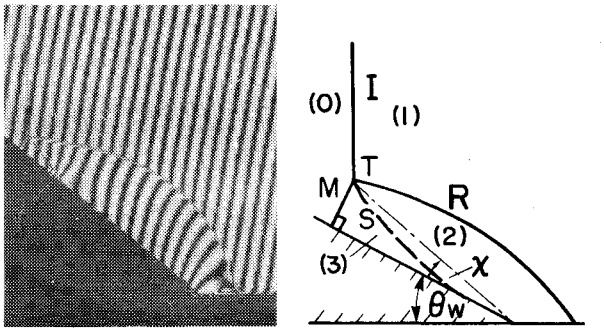

b) Single-Mach reflection (SMR), $\theta_w = 40$ deg, $M_s = 2.10$.

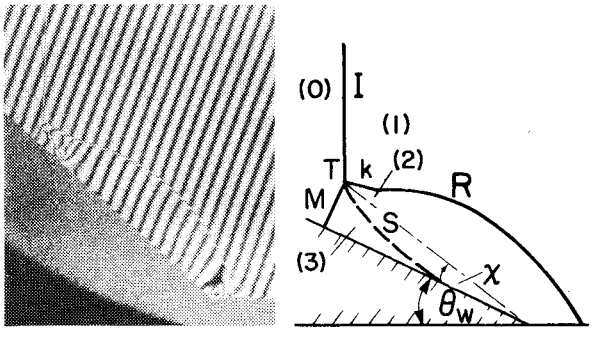

c) Complex-Mach reflection (CMR), $\theta_w = 40$ deg, $M_s = 2.59$.

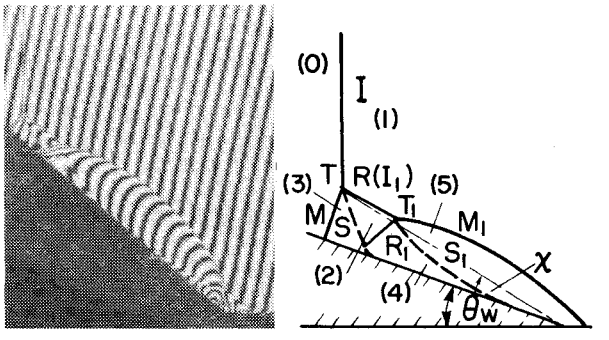

d) Double-Mach reflection (DMR), $\theta_w = 40$ deg, $M_s = 4.78$.

Fig. 1 Illustration of four possible oblique shock-wave reflections. The interferograms ($\lambda = 6943$ Å) were taken with a 23-cm-diam Mach-Zehnder interferometer in the 10 × 18-cm UTIAS Hypervelocity Shock Tube for oxygen at an initial pressure $P_0 \simeq 15$ Torr and temperature $T_0 \simeq 300$ K.

Table 1 Various reflection cases and their initial conditions

Type	Case	Initial conditions[a]	Imperfect gas: Present experiment	Perfect gas: Schneyer[21] Eulerian	Perfect gas: Schneyer[21] Lagrangian	Perfect gas: Kutler and Shankar[22]
Regular reflection	1	Gas	N_2	$\gamma = 1.40$	...	$\gamma = 1.40$
		θ_w, deg	63.43	63.43	...	63.41
		M_s	2.01	2.00	...	2.00
		P_0, Torr	50.00	760	...	760
		T_0, K	298.6	...	...	...
		ρ_0, g/cm^3	7.57×10^{-5}	10^{-3}	...	10^{-3}
Regular reflection	2	Gas	N_2	...	...	O_2
		θ_w, deg	60.00	...	...	60
		M_s	4.68	...	...	4.71
		P_0, Torr	15.31	...	...	15
		T_0, K	298.1	...	...	298.6
		ρ_0, g/cm^3	2.31×10^{-5}	...	...	2.50×10^{-5}
Single-Mach reflection	3	Gas	N_2	$\gamma = 1.40$	$\gamma = 1.40$	...
		θ_w, deg	26.56	26.56	26.56	...
		M_s	2.01	2.00	2.00	...
		P_0, Torr	50.00	...	...	...
		T_0, K	296.6	...	...	...
		ρ_0, g/cm^3	7.57×10^{-5}	10^{-3}	10^{-3}	...

[a] Initial conditions are for the quiescent gas ahead of the incident shock wave.

interferometer was used for recording the nonstationary process. The light source consisted of a giant-pulse ruby laser. Simultaneous dual-frequency interferograms were taken at wavelengths of 6943 and 3471.5 Å, respectively. The interferograms were evaluated using a very precise method developed by Whitten.[25] The identical equipment and evaluation methods were used recently to study ionized shock structure, sidewall boundary layers, and flat-plate boundary layers in ionizing argon flows. The reflection errors were found to be unimportant.[25-28] In both investigations, very satisfactory to good agreement was obtained using quite sophisticated numerical methods. Consequently, the gross inviscid flowfields from the present experiments and those of Refs. 21-23 can be compared with confidence.

All of the isopycnics in the figures are numbered, and the corresponding values of ρ/ρ_0 as well as the absolute accuracy in evaluating the density from the interferograms are listed in each figure. The isopycnics are drawn in the (x,y) plane within an accuracy of ± 1 mm. Figure 1 illustrates with actual interferograms and line drawings (for clarity) in order to define the wedge angles θ_w, the triple point trajectories χ, and the various shock waves, slipstreams, and flow regions produced by RR (Fig. 1a), SMR (Fig. 1b), CMR (Fig. 1c), and DMR (Fig. 1d).

Comparison with Some Numerical Data and Discussions

The different compared cases and their initial conditions are shown in Table 1. Although we have tried to perform our new experiments using exactly the same initial conditions as those chosen by Schneyer and Kutler and Shankar for their numerical analyses, it was experimentally convenient to use nitrogen at different initial pressures. However, because nitrogen and oxygen can be treated as perfect gases at a shock Mach number $M_s = 2.00$, the change in the initial pressure was not significant. Furthermore, since the values of the flow isopycnics were normalized by the initial density ahead of the incident shock wave, any correctly computed and actual isopycnic shapes and values must be the same. However, for strong shock waves real-gas effects are important and must be taken into account for RR at $M_s = 4.68$ and $P_0 = 15.31$ Torr.

It can be seen from Table 1 that three different cases were compared. Case 1 results in an RR with a weak incident shock wave ($M_s = 2.0$), and it was solved numerically by Schneyer and Kutler and Shankar. Case 2 is again an RR but with a stronger incident shock wave ($M_s = 4.71$), and it was analyzed by Kutler and Shankar. Case 3, an SMR, was solved by Schneyer using two different computer codes: the two-dimensional Eulerian code THOR, a revised version of the HELP[29] code, and the two-dimensional Lagrangian code CRAM, based on Wilkins'[30] formulation. In Ref. 22, the two-dimensional time-dependent Euler equations were solved. The hyperbolic partial-differential equations were transformed to introduce self-similarity, and the distance between the corner and the incident shock wave was used for normalization. The self-similar transformation reduces these equations from an unsteady to a quasisteady set of mixed elliptic-hyperbolic equations. Then the equations were made totally hyperbolic by reintroducing a timelike term. The final set of equations was written in a "strong conservation law form" and solved using MacCormack's[31] second-order finite-difference algorithm.

Comparison with Case 1

The shapes of the isopycnics obtained numerically by Schneyer, Kutler and Shankar, and in the present experiments are shown in Figs. 2a-2c, respectively. The actual interferogram appears in Fig. 2d. The contour number and the corresponding density ratio are tabulated in Figs. 2a and 2c. Unfortunately, we were unable to obtain the contour numbers from Kutler and Shankar for Fig. 2b. It is worth noting that our measured density ratios immediately behind the incident and reflected shock waves always agree well with theory. It can be seen immediately that the actual shapes of the isopycnics obtained experimentally appear similar to those predicted by Kutler and Shankar. However, the results from Schneyer do not represent the physical flow. One could discard the isopycnics shown by Schneyer using the following argument. Schneyer's isopycnics (even if their lines were taken to represent the shock as a result of artificial viscosity smearing) have the same value over the entire length of the reflected shock R. This means that the density jump across R is constant everywhere. However, since the angle of incidence between the flow entering R (in a frame of reference attached to the reflection point P) decreases as R moves away from P, the strength of R should increase to maintain a constant density jump. This contradicts both theory and experiment, where the shock-wave strength along R decreases as the distance from the reflection point increases, as shown in Fig. 2c. Consequently, the density ratios in the vicinity of Q in Fig. 2a are much larger compared with the actual result (Fig. 2c). However, just the range of density given by Schneyer (Fig. 2a) approximates the measured range (Fig. 2c). Unfortunately, only a qualitative comparison can be made with the results of Kutler and Shankar, since their values corresponding to the various isopycnics were not given on the figures in Ref. 22 and were unavailable from private communications.

A comparison between the actual shock-wave configuration and the shapes predicted by Schneyer and Kutler and Shankar is shown in Fig. 2e. Since several isopycnics of Schneyer represent shock waves as a result of artificial viscosity, the two extreme contours were reproduced in Fig. 2e. The distance between the incident shock wave and the corner is normalized for all shapes. It can be seen clearly from Fig. 2e that the predicted shapes do not differ too much from the actual shock-wave configuration. It is worth mentioning that Kutler and Shankar predict their numerically-obtained configuration to be slightly larger than the actual one. However, their explanation that this is due to viscous or real-gas effects is reasonable for the latter. It can be shown analytically that vibrational excitation will reduce the angle between the reflected shock wave and the wedge and hence will result in a smaller configuration. The angle between R and the wedge surface at the reflection point is 16.34 deg for a perfect gas and 16.04 deg when real-gas effects are considered. Note that, although Schneyer and Kutler and Shankar used two different computational methods that disagree in the prediction of the entire density field, they nevertheless agree in the shock shapes and systems. One can conclude only that the isopycnics are much more sensitive indicators of the accuracy of the physical flow modeled by a specific numerical technique.

Comparison with Case 2

The general shapes of the isopycnics predicted by Kutler and Shankar (Fig. 3a) do not agree with the actual ones (Fig. 3b). Their predicted shapes for this case of RR are almost the same as those discussed previously (Fig. 2b), whereas our results are very different (Fig. 2c). The disagreement between the actual and numerical isopycnics may arise from the following:

1) Although this case, as well as the one discussed previously, is of the RR type, the diffraction processes are different.[24] In case 1, the flow behind the incident shock wave (in laboratory coordinates) was subsonic ($M_2 = 0.97$), and it readily turned the corner to interact with the shock-wave reflection process. However, in case 2 the flow behind the incident shock wave was supersonic ($M_2 = 1.78$). Consequently, it could turn the corner subsonically only after passing through a detached shock wave. (If there was no interaction with the boundary layer, the flow Mach number behind the normal portion of the shock would be 0.62.) Since this diffraction process is different from the one discussed previously, the resulting flowfields must exhibit a different density pattern. It should be noted that the detached shock wave (Fig. 3c) interacts with an already-existing boundary layer induced by the incident shock wave. However, Fig. 2d does not show this kind of intense interaction where a detached shock wave is absent.

2) Kutler and Shankar assume a perfect gas. However, for $M_s = 4.71$, $P_0 = 15$ Torr, $T_0 = 298.6$ K, real-gas effects cannot be neglected, as the vibrational contribution is significant (e.g., $\rho_2/\rho_0 = 14.53$ for a perfect gas and 17.75 for an imperfect gas). Although this will change the absolute numerical vaues of the isopycnics, it also might affect their shapes.

3) They also assume that the reflection (or diffraction) phenonemon is self-similar. However, when a planar shock wave moves over a wedge in a constant-area shock tube, it will accelerate somewhat because of the convergence of the cross section caused by the wedge,[32-33] as verified by our shock-wave-velocity measurements. This may not affect the analysis seriously, but it should not be overlooked.

Although Kutler and Shankar did not report the values of the various isopycnics on their reproduced Fig. 3a, we deduced representative values from their density distribution along the wall shown in Fig. 3d. The range of their densities is lower than ours because of their assumption of a perfect gas. Note that the strength of the reflected shock wave R decreases from the reflection point to the shock-tube wall, in agreement

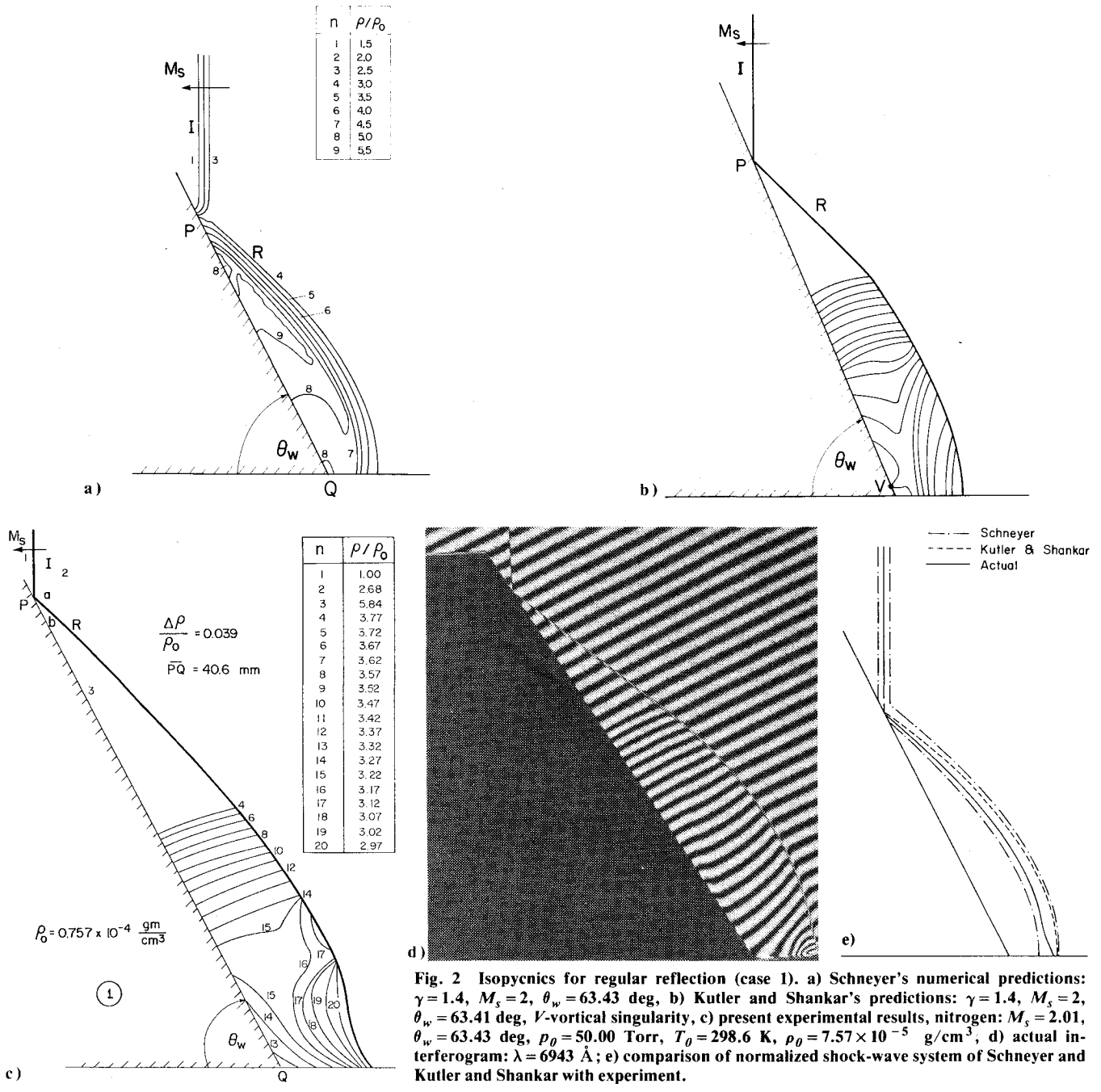

Fig. 2 Isopycnics for regular reflection (case 1). a) Schneyer's numerical predictions: $\gamma = 1.4$, $M_s = 2$, $\theta_w = 63.43$ deg, b) Kutler and Shankar's predictions: $\gamma = 1.4$, $M_s = 2$, $\theta_w = 63.41$ deg, V-vortical singularity, c) present experimental results, nitrogen: $M_s = 2.01$, $\theta_w = 63.43$ deg, $p_0 = 50.00$ Torr, $T_0 = 298.6$ K, $\rho_0 = 7.57 \times 10^{-5}$ g/cm^3, d) actual interferogram: $\lambda = 6943$ Å; e) comparison of normalized shock-wave system of Schneyer and Kutler and Shankar with experiment.

with experiment (Fig. 3b.) The numerically calculated density distribution along the wall surface predicted by Kutler and Shankar and the measured values close to the wall above the thin boundary layer are shown in Figs. 3d and 3e, respectively. The fact that the actual density values are higher than those predicted by Kutler and Shankar again arises from their perfect-gas assumption. For their case of $M_s = 4.71$, the perfect-gas value $\rho_2/\rho_0 = 14.53$, whereas, for our case the measured value of $\rho_2/\rho_0 = 16.77$, and it lies between the perfect and imperfect equilibrium values of 14.48 and 17.65, respectively.

The vortical singularity V predicted by Kutler and Shankar (Fig. 3a) or point d (Fig. 3d) cannot be seen in the interferogram. Therefore, the curve from b to f (Fig. 3e), unlike the curve in Fig. 3d, has no discontinuity. If one existed, it would be smeared out by the boundary layer. Both curves consist of a sharp density jump ρ_{20} (f-f) at the reflection point, followed by a uniform density region (which is longer in Fig. 3d) terminated by an expansion. At the detached shock wave position b, another sharp rise takes place. (The rise is greater in Fig. 3d.) The fringe pattern due to the shock-boundary-layer interaction at the corner was too complex to analyze. Therefore, the density ratio was extrapolated to the location of the detached shock wave near the corner.

The actual shock-wave configuration and the one predicted by Kutler and Shankar are shown in Fig. 3f. This figure agrees with their statement that "the experimental shock location would fall inside the numerical solution." As mentioned earlier, the reason for this lies in real-gas effects rather than viscous effects suggested by Kutler and Shankar. The angle between the reflected shock wave R and the wedge surface for a perfect gas is 14.80 deg and for a real gas is 12.45 deg. Consequently, the actual shape is smaller than the one obtained from a perfect-gas model.

The measured density distribution along the wall corresponding to case 1 appears on Fig. 3g. A comparison of the density distributions for cases 1 and 2, shown in Figs. 3g and 3e, respectively, reveals immediately that the two dif-

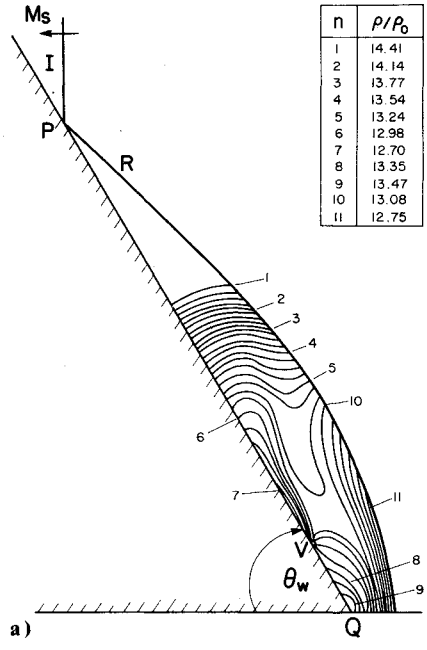

n	ρ/ρ_0
1	14.41
2	14.14
3	13.77
4	13.54
5	13.24
6	12.98
7	12.70
8	13.35
9	13.47
10	13.08
11	12.75

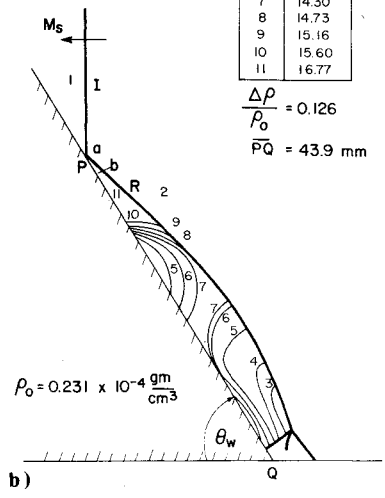

n	ρ/ρ_0
1	1.00
2	5.32
3	12.57
4	13.00
5	13.43
6	13.86
7	14.30
8	14.73
9	15.16
10	15.60
11	16.77

$\frac{\Delta\rho}{\rho_0} = 0.126$

$\overline{PQ} = 43.9$ mm

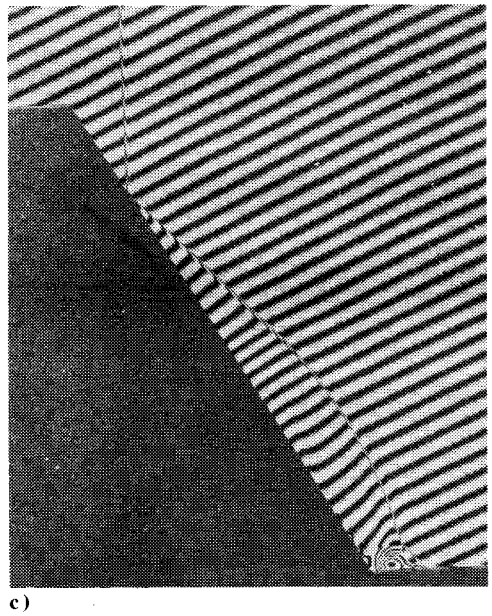

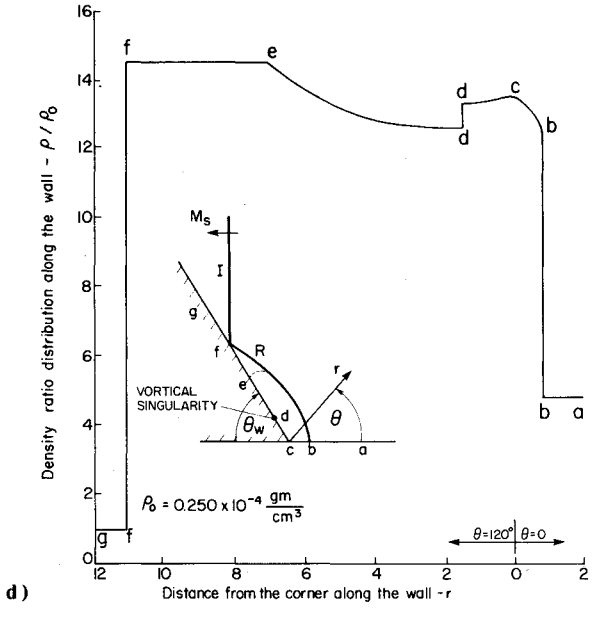

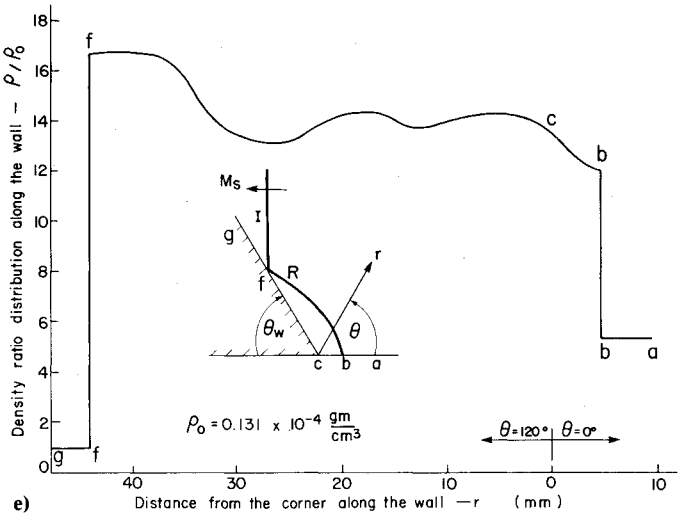

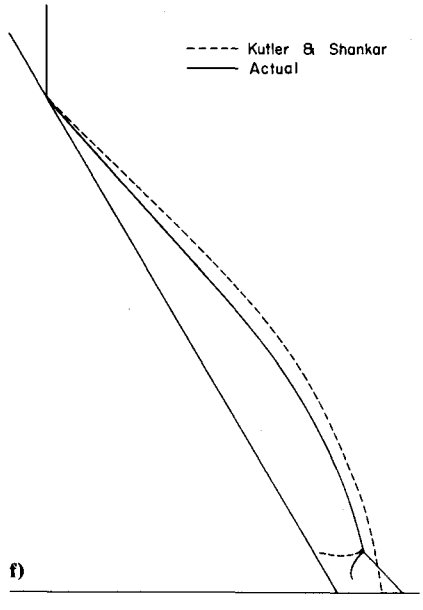

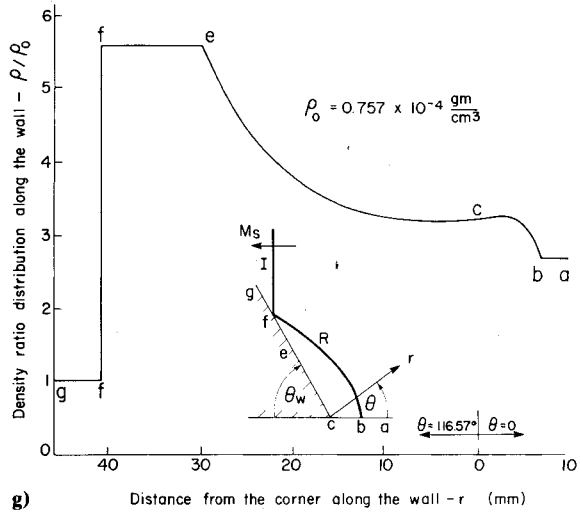

Fig. 3 Isopycnics for regular reflection (case 2). a) Kutler and Shankar's numerical predictions, oxygen: $\gamma = 1.4$, $\theta_w = 60.00$ deg, $M_s = 4.71$; b) present experimental results, nitrogen: $M_s = 4.68$, $\theta_w = 60$ deg, $p_0 = 15.31$ Torr, $T_0 = 298.1$ K; c) actual interferogram: $\lambda = 6943$ Å; d) Kutler and Shankar's density distribution along the wall; e) present experimental density distribution along the wall surface for conditions in Fig. 3b; f) comparison of normalized shock-wave system of Kutler and Shankar with experiment; g) present experimental density distribution along the wall for regular reflection (case 1), nitrogen: $M_s = 2.01$, $\theta_w = 63.43$ deg, $p_0 = 50.00$ Torr, $T_0 = 298.6$ K, $\rho_0 = 7.57 \times 10^{-5}$ g/cm^3.

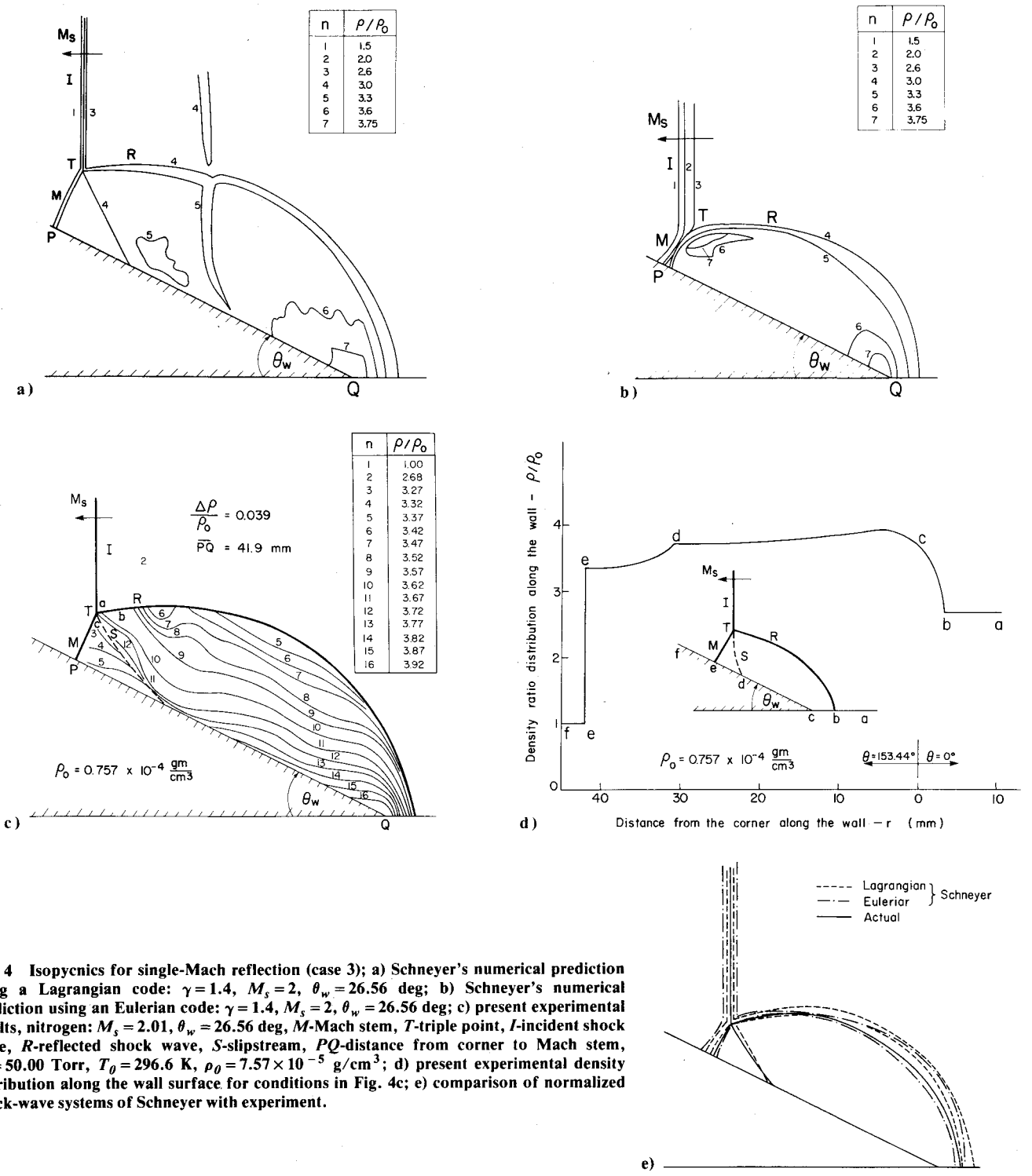

Fig. 4 Isopycnics for single-Mach reflection (case 3); a) Schneyer's numerical prediction using a Lagrangian code: $\gamma = 1.4$, $M_s = 2$, $\theta_w = 26.56$ deg; b) Schneyer's numerical prediction using an Eulerian code: $\gamma = 1.4$, $M_s = 2$, $\theta_w = 26.56$ deg; c) present experimental results, nitrogen: $M_s = 2.01$, $\theta_w = 26.56$ deg, M-Mach stem, T-triple point, I-incident shock wave, R-reflected shock wave, S-slipstream, PQ-distance from corner to Mach stem, $p_0 = 50.00$ Torr, $T_0 = 296.6$ K, $\rho_0 = 7.57 \times 10^{-5}$ g/cm^3; d) present experimental density distribution along the wall surface for conditions in Fig. 4c; e) comparison of normalized shock-wave systems of Schneyer with experiment.

fraction processes are different, as mentioned earlier, whereas in case 2 the presence of a detached shock wave is clearly seen at *b-b* (density ratio of 2.24). There is no evidence that a bow shock exists in case 1, where the density increases through a smooth compression from *b* to *c*. This fact indicates that the rarefaction wave generated at the corner *c* overtakes the reflected shock wave *R*, bends it back, and weakens it until it degenerates into a Mach wave.

Comparison with Case 3

The shapes of the isopycnics obtained numerically by Schneyer[21] using the Lagrangian and Eulerian computer codes, as well as those obtained experimentally, are shown in Figs. 4a-4c, respectively. It is evident that the Lagrangian and Eulerian results differ quite considerably from each other and from the actual isopycnics. The numerical configurations suffer from the same artificially viscous spreading of the incident and reflected shock waves. The fact that the isopycnics maintain the same value along *R* implies a physically unrealistic reflected shock wave of increasing strength as it moves away from the triple point *T*. Spurious isopycnics ($n = 4$ and 5, Fig. 4a) appear from the Lagrangian code in the middle of the reflected wave *R*. There are no density contours generated in the important region between the Mach stem *M* and the slipstream *S*. The Eulerian contours fail to predict the existence of a slipstream altogether (Fig. 4b). If a line is drawn at the estimated location of the slipstream, it intersects the isopycnics, implying that the densities

on both sides of the slipstream are equal, in violation of the physical condition that the slipstream divides two thermodynamic regions of different densities, even if not large. Schneyer[21] attributes the appearance of the spurious expansion and shock waves in the middle of R in the Lagrangian results to an inexact choice of the initial velocity profile. He explains the disappearance of the slipstream (in the Eulerian result) as being "washed out" by the "effective (artificial) viscosity."

The actual shape of the isopycnics (Fig. 4c) shows very clearly that the densities on both sides of the slipstream are different. The densities behind the reflected shock wave are higher than those behind the Mach stem, as expected from gasdynamic considerations. The approximate density ratio across the slipstream is 1.12 (3.67/3.27 near the triple point), which shows that it is indeed a weak discontinuity. The analytical density ratio across the slipstream in the vicinity of the triple point is 1.10. A qualitative comparison between the shapes of the actual isopycnics and those of Schneyer indeed show poor agreement. However, as in the previous case, only the range of density values approximates those obtained experimentally.

It is worth noting the convergence of the isopycnics toward the reflected shock wave at R (Fig. 4c). This indicates the existence of a weak expansion wave. The density ratio across it was 0.96 (3.42/3.51). (Note that an expansion wave was predicted by the Lagrangian code.) It was shown[24] that, at higher incident shock-wave Mach numbers M_s, the expansion wave is replaced by a compression wave forming a CMR; that is, a kink occurs in the reflected wave R at the point where the isopycnics converge. For even higher values of M_s, the compression wave converges to form a shock wave, giving rise to a DMR.

The density distribution close to the wall surface for this case is shown in Fig. 4d. Since $M_s = 2.01$ (i.e., $M_s < 2.068$), the flow behind the incident shock wave is subsonic. Therefore, it turns the corner subsonically, and the reflected wave again degenerates to a Mach wave and a compression b-c. The flow passing through the Mach stem is compressed further (e-d). A mild discontinuity appears at d, where the slipstream disappears near the wall. The density jump across the Mach stem (within 0.5 mm, as close as it is possible to evaluate the fringes) increases from the triple point T to the wall P (Fig. 4c). Consequently, the Mach stem is curved (slightly concaved toward the slipstream).

A comparison between the normalized predicted shock shapes and the actual wave configuration is shown in Fig. 4e. The Lagrangian wave system is somewhat larger than the Eulerian. The actual shock-wave system lies close to or inside the Eulerian shape boundaries. The slipstream predicted by the Lagrangian code agrees reasonably well with experiment. It is worth repeating that also in this case the Lagrangian and Eulerian codes predict the actual wave system quite well. However, isopycnic fields and the varying strength of the reflected wave are poorly represented. Many additional details can be found in Refs. 24 and 34.

Conclusions

Some comprehensive interferometric data are presented on nonstationary regular and single-Mach reflections of shock waves in real nitrogen. These results are the first of their kind since the pioneering work of White[8] in 1951. They form a base from which the accuracy of existing numerical experiments with identical initial conditions can be assessed.

Kutler and Shankar[22] have reviewed the existing computational analyses in the U.S. and the USSR. Our experiments reported here and elsewhere[24,34] show that all numerical methods provide reasonable predictions of the wave systems and their shapes for the two analyzed cases of RR and SMR. No numerical data exist for the case of CMR and DMR. The numerical codes predict rather poor values and locations for the more sensitive indicators of the flow properties, namely, the isopycnics. Of the various numerical analyses produced so far, the ones of Kutler and Shankar[22] and Shankar et al.[23] are superior. Even their codes require a reassessment and perhaps a new approach in the light of the disagreement with the detailed and very accurate interferometric data presented here.

Undoubtedly, numerical codes will evolve in the future which will reliably predict not only RR and SMR but also CMR and DMR in real gases. Our interferometric data of all of these cases[24] should provide a solid base for comparison. In the meantime, those laboratories that have shock tubes equipped with interferometers will benefit from experiments in nonstationary flows in order to check their numerical analyses. Further details are given in Refs. 24 and 34.

Acknowledgments

We wish to thank C. K. Law for helping us to reinitiate and to extend his M.A.Sc. research at the University of Toronto Institute for Aerospace Studies. The constructive review of our work by S. Molder is appreciated. The financial assistance from the National Research Council of Canada and the U.S. Air Force under Contract AF-AFOSR 77-3303 is gratefully acknowledged.

References

[1] Seeger, R. J. and Polacheck, H., "Regular Reflections of Shocks in Ideal Gases," Navy Dept., Bureau of Ordnance, Re2c, Washington, D.C., Explosive Research Rept. 13, 1943.

[2] von Neumann, J., "Oblique Reflection of Shocks," Navy Dept., Bureau of Ordnance, Re2c, Washington, D.C., Explosive Research Rept. 12, 1943.

[3] von Neumann, J., "Refraction, Intersection and Reflection of Shock Waves," Navy Dept., Bureau of Ordnance, Washington, D.C., NAVORD Rept. 203-45, 1945.

[4] Smith, L. G., "Photographic Investigation of the Reflection of Plane Shocks in Air," Office of Scientific Research and Development, Washington, D.C., Rept. 4943, 1945.

[5] Taub, A. H., "Refraction of Plane Shock Waves," *Physical Review*, Vol. 72, July 1947, pp. 51-60.

[6] Bleakney, W. and Taub, A. H., "Interaction of Shock Waves," *Review of Modern Physics*, Vol. 21, Oct. 1949, pp. 584-605.

[7] Fletcher, C. H., "The Mach Reflection of Weak Shock Waves," Dept. of Physics, Princeton Univ., TR II-4, 1951.

[8] White, D. R., "An Experimental Survey of the Mach Reflection of Shock Waves," Dept. of Physics, Princeton Univ., TR II-10, 1951.

[9] Jahn, R. G., "The Refraction of Shock Waves at Gaseous Interface, Regular Refraction of Weak Shocks; Regular Refraction of Strong Shocks; Irregular Refraction," Dept. of Physics, Princeton Univ., TR II-16, 1954; II-18, 1955; and II-19, 1956.

[10] Kawamura, R. and Saito, H., "Reflection of Shock Waves—I, Pseudo Stationary Case," *Journal of the Physical Society of Japan*, Vol. 11, May 1956, pp. 584-592.

[11] Molder, S., "Head-On Interaction of Oblique Shock Waves," Univ. of Toronto, UTIAS TN 38, 1960; also "Shock Reflection and Interaction at Hypersonic Speeds," *Journal of Spacecraft and Rockets*, Vol. 1, Nov.-Dec., 1964, pp. 688-689.

[12] Henderson, L. F., "On the Confluence of Three Shock Waves in a Perfect Gas," *Aeronautical Quarterly*, Vol. XV, May 1964, pp. 181-197.

[13] Gvozdeva, L. G., Bazhenova, T. V., Predvoditeleva, O. A., and Fokeev, V. P., "Mach Reflection of Shock Waves in Real Gases," *Aeronautica Acta*, Vol. 14, May 1967, pp. 503-508.

[14] Law, C. K. and Glass, I. I., "Diffraction of Strong Shock Waves by a Sharp Compressive Corner," *CASI Transactions*, Vol. 4, Jan. 1971, pp. 2-12.

[15] Skews, B. W., "The Flow in the Vicinity of a Three-Shock Intersection," *CASI Transactions*, Vol. 4, Feb. 1971, pp. 99-107.

[16] Skews, B. W., "The Effect of an Angular Slipstream on Mach Reflection," McMaster Univ., Hamilton, Ontario, 1971.

[17] Skews, B. W., "The Deflection Boundary Condition in the Regular Reflection of Shock Waves," McMaster Univ., Hamilton, Ontario, 1972.

[18] Henderson, L. F. and Lozzi, A., "Experiments on Transition of Mach Reflection," *Journal of Fluid Mechanics*, Vol. 68, Pt. 1, March 1975, pp. 139-155.

[19]Bazhenova, T. V., Fokeev, V. P., and Gvozdeva, L. G., "Regions of Various Forms of Mach Reflection and Its Transition to Regular Reflection," *Acta Astronautica*, Vol. 3, Jan.-Feb. 1976, pp. 131-140.

[20]Hornung, H. G. and Kychakoff, G., "Transition from Regular to Mach Reflection of Shock Waves in Relaxing Cases," *Proceedings of the 11th International Shock Tube Symposium*, Univ. of Washington, Seattle, Wash., 1977.

[21]Schneyer, G. P., "Numerical Simulation of Regular and Mach Reflections," *The Physics of Fluids*, Vol. 18, Sept. 1975, pp. 1119-1124.

[22]Kutler, P. and Shankar, V. S., "Diffraction of a Shock Wave by a Compression Corner: I. Regular Reflection," *AIAA Journal*, Vol. 15, Feb. 1977, pp. 197-202.

[23]Shankar, V. S., Kutler, P., and Anderson, D. A., "Diffraction of Shock Waves by a Compression Corner, Part II—Single Mach Reflection," AIAA Paper 77-89, 1977.

[24]Ben-Dor, G. and Glass, I. I., "Domains and Boundaries of Nonstationary Oblique Shock-Wave Reflection: I—Diatomic Gas," (to be published in the *Journal of Fluid Mechanics*).

[25]Whitten, B. T., "An Interferometric Investigation of Quasi-Steady Shock-Induced Boundary Layers in Partially Ionized Argon," Univ. of Toronto, UTIAS Rept. (to be published); also Tang, F. C., "Effects of Impurities on Shock Wave Stability and Structure in Ionizing Monatomic Gases," Univ. of Toronto, UTIAS TN 212, Nov. 1977.

[26]Glass, I. I., and Liu, W. S., "Effects of Hydrogen Impurities on Shock Structure and Stability in Ionizing Monatomic Gases, Part 1: Argon," *Journal of Fluid Mechanics*, Vol. 84, Pt. 1, Jan. 1978, pp. 55-77.

[27]Glass, I. I., Liu, W. S., and Tang, F. C., "Effects of Hydrogen Impurities on Shock Structure and Stability in Ionizing Monatomic Gases, Part 2: Krypton," *Canadian Journal of Physics*, Vol. 55, No. 14, July 1977, pp. 1269-1279.

[28]Liu, W. S., Whitten, B. T., and Glass, I. I., "Ionizing Boundary Layers: 1. Quasi-Steady Flat-Plate Laminar Boundary-Layer Flows," *Journal of Fluid Mechanics*, Vol. 87, 1978, p. 609 (to be published).

[29]Hageman, L. J. and Walsh, J. M., "HELP, a Multi-Material Eulerian Program for Compressible Fluid and Elastic-Plastic Flows in Two Space Dimensions and Time," Ballistic Research Laboratories, BRL Contract Rept. No. 39, May 1971.

[30]Wilkins, M. L., "Calculation of Elastic-Plastic Flow," *Methods in Computational Physics*, Vol. 3, by B. Alder, S. Fernbach, and M. Rothenberg, Academic Press, New York, 1964, p. 211.

[31]MacCormack, R. W., "The Effect of Viscosity in Hypervelocity Impact Cratering," AIAA Paper 69-354, 1969.

[32]Higashimo, F. and Oshima, N., "Real Gas Effects on Converging Shock Waves," *Astronautica Acta*, Vol. 15, Nov. 1970, pp. 523-529.

[33]Russell, D. A., "Shock Wave Strengthening by Area Convergence," *Journal of Fluid Mechanics*, Vol. 27, Pt. 2, Feb. 1967, pp. 305-314.

[34]Ben-Dor, G., "Regions and Transitions of Nonstationary Oblique Shock-Wave Diffractions in Perfect and Imperfect Gases," UTIAS Rept. No. 232, Aug. 1978.